Comparative study of structural, electronic and optical properties of Ca_2Si, Ca_2Ge, Ca_2Sn, and Ca_2Pb

D. B. Migas* and Leo Miglio

INFM and Dipartimento di Scienza dei Materiali, Università di Milano-Bicocca, via Cozzi 53, 20125 Milano, Italy

V. L. Shaposhnikov and V. E. Borisenko

Belarusian State University of Informatics and Radioelectronics, P. Browka 6, 220013 Minsk, Belarus

We report *ab initio* results for the ground-state properties, band diagrams, density of states, and dielectric functions of Ca_2Z (Z=Si, Ge, Sn, and Pb) both in the orthorhombic and cubic structures. The calculations are performed by means of total energy ultrasoft pseudopotential and full potential linearized augmented plane wave methods within local density and generalized gradient approximations. The estimated difference in the cohesion energy shows the orthorhombic structure to be the stable phase. We also demonstrate that these materials are semiconductors independently of the phase. A direct energy gap and sizable anisotropy in optical spectra characterize orthorhombic Ca_2Z, whereas a competitive direct-indirect character of the gap and a high value of oscillator strength of the first direct transition are predicted for cubic Ca_2Z.

I. INTRODUCTION

New semiconducting materials technologically compatible with silicon and germanium are of practical importance for the design of novel electronic devices. Silicides and germanides indeed look attractive and their properties are still mainly studied for transition metal compounds.[1,2] Some attention was also paid to compounds of silicon with alkaline-earth metals (namely, Mg, Ca, Ba), where only two silicides Mg_2Si and $BaSi_2$ were previously reported to be semiconductors,[1] while contradictory data exist for Ca_2Si. Properties of other calcium compounds such as Ca_2Ge, Ca_2Sn, and Ca_2Pb are either unknown or limited by few dispersed notes. X-ray powder diffraction analyses[3–9] of Ca_2Z (Z stands for Si, Ge, Sn, and Pb) compounds reveal the simple orthorhombic structure and no evidence of a cubic phase reported in some old researches[10] is found. Theoretical calculations by the linear muffin-tin orbital method[11] indicated Ca_2Si to be a semimetal. However, this point is not definitely confirmed by the photoemission[11] and inverse-photoemission[12] experiments. On the other hand a gap of 1.90 eV is reported on the basis of resistivity measurements[10] and very recent pseudopotential calculations[13] predict its value to be 0.36 eV. The energy gap of 0.90 and 0.46 eV have been estimated for Ca_2Sn and Ca_2Pb, respectively.[10] Semiconducting properties are also confirmed in the case of Ca_2Sn by resistivity experiments[3] still the value of the gap is not reported. To our knowledge there is no information about Ca_2Ge and no data on optical properties of Ca_2Z are available.

Taking into account rather scarce and in some cases contradictory data, it is important to perform a systematic theoretical study of Ca_2Z in order to estimate the energy difference between orthorhombic and cubic phases (which of them is lower at 0 K and whether this is true for any compound) and then to trace changes in electronic and optical properties with respect to the phase and Z. For the first goal it is useful to apply the ultrasoft pseudopotential method perfectly suitable for a total energy calculation and a full structural optimization, whereas for the second goal the full potential linearized augmented plane wave method meets the adequate requirements.

II. MODEL AND COMPUTATIONAL METHODS

A. Crystal structure

The Ca_2Z compounds possess a simple orthorhombic crystalline structure (the *Pnma* space group[3–9]) and their lattice parameters are listed in Table I. The primitive cell contains four formula units where 12 atoms are grouped into three equal sets (Ca1, Ca2, Z) of chemically inequivalent sites. In Fig. 1 we show the orthorhombic unit cell in comparison with the cubic one (the antifluorite structure in which the Mg_2Z compounds crystallize). In this cubic structure each Z atom is surrounded by a cubic cage of the Ca atoms which transforms into tricapped trigonal prisms in the orthorhombic structure.[3] Nevertheless some similarities in the two structures can be traced. Thus, by the dashed line (Fig. 1, left panel) we indicate a cell which resembles the cubic one (Fig. 1, middle panel) where the Z subcage is shifted up by $b/4$ with some displacement of the middle row along z while the Ca subcage is distorted in the (010) plane. On the contrary, a crucial displacement of the atoms is evident in the (100) plane of the orthorhombic structure (Fig. 1, right panel) with respect to the cubic one.

B. Details of the calculations

For total energy calculation and full structural optimization we have applied the first principles code VASP (Vienna *ab initio* simulation package) with the plane-wave basis set and ultrasoft pseudopotentials (USPP) described in detail elsewhere.[14–16] Exchange and correlation potentials were included either using the local density approximation (LDA) of Ceperly and Alder by the parameterization of Perdew and

TABLE I. Optimized lattice constants a, b, and c (Å), equilibrium volume V_0 (Å^3/f.u.), cohesion energy E_{coh} (eV/f.u.) and bulk modulus B_0 (Mbar) of orthorhombic and cubic Ca$_2$Z.

		a	b	c	V_0	E_{coh}	B_0
Ca$_2$Si	cubic$_{LDA}$	7.016			86.34	11.766	0.41
	orthorhombic$_{LDA}$	7.355	4.726	8.856	76.96	11.886	0.46
	orthorhombic$_{exp}$ [a]	7.667	4.799	9.002	82.80		
	orthorhombic$_{exp}$ [b]	7.691	4.816	9.035	83.66		
	orthorhombic$_{GGA}$	7.618	4.793	9.001	82.16	10.773	0.40
	cubic$_{GGA}$	7.148			91.30	10.740	0.37
Ca$_2$Ge	cubic$_{LDA}$	7.035			87.04	11.490	0.40
	orthorhombic$_{LDA}$	7.418	4.747	8.869	78.08	11.607	0.44
	orthorhombic$_{exp}$ [a]	7.734	4.834	9.069	84.76		
	orthorhombic$_{exp}$ [c]	7.715	4.821	9.058	84.23		
	orthorhombic$_{exp}$ [c]	7.715	4.832	9.067	84.50		
	orthorhombic$_{GGA}$	7.665	4.834	9.058	83.91	10.353	0.38
	cubic$_{GGA}$	7.197			93.20	10.311	0.35
Ca$_2$Sn	cubic$_{LDA}$	7.386			100.73	10.881	0.36
	orthorhombic$_{LDA}$	7.146	5.142	9.350	85.89	11.055	0.41
	orthorhombic$_{exp}$ [d]	7.975	5.044	9.562	96.16		
	orthorhombic$_{exp}$ [e]	7.981	5.043	9.566	96.25		
	orthorhombic$_{exp}$ [f]	7.992	5.037	9.554	96.15		
	orthorhombic$_{GGA}$	7.924	5.050	9.586	95.90	9.789	0.35
	cubic$_{GGA}$	7.556			107.85	9.708	0.28
Ca$_2$Pb	cubic$_{LDA}$	7.440			102.96	10.398	0.34
	orthorhombic$_{LDA}$	7.204	5.209	9.401	88.19	10.581	0.39
	orthorhombic$_{exp}$ [a, e]	8.072	5.100	9.647	99.28		
	orthorhombic$_{exp}$ [g]	8.035	5.067	9.617	97.89		
	orthorhombic$_{GGA}$	8.005	5.124	9.665	99.11	9.291	0.34
	cubic$_{GGA}$	7.621			110.66	9.135	0.28

[a]Reference 4.
[b]Reference 6.
[c]Reference 9.
[d]Reference 5.
[e]Reference 3.
[f]Reference 7.
[g]Reference 8

Zunger,[17] or the generalized gradient approximation (GGA) of Perdew and Wang.[18] The ultrasoft Vanderbilt-type pseudo-potentials have been employed for the $3p^6 4s^2 4d^0$, $3s^2 3p^2$, $4s^2 4p^2$, $4d^{10} 5s^2 5p^2$, and $5d^{10} 6s^2 6p^2$ atomic configurations of Ca, Si, Ge, Sn, and Pb, respectively, where the Ca $3p^6$, Sn $4d^{10}$, and Pb $5d^{10}$ semicore states were treated as valence states. The linear tetrahedron method with Blöchl corrections has been applied for the Brillouin zone (BZ) integration. Total energy minimization, via an optimization of the lattice parameters and a relaxation of the atomic positions in a conjugate gradient routine, was obtained by calculating the Hellmann-Feynman forces and the stress tensor. The Pulay corrections have been included in order to compensate for changes of the basis set due to a variation in the shape of the unit cell. The convergence in the total energy for both phases was better than 1 meV/atom using the energy cutoff of 400 eV and the $6 \times 8 \times 4$ grid of Monkhorst-Pack points for the orthorhombic phase and the $11 \times 11 \times 11$ one for the

cubic phase. The calculation of band structures along some high symmetry directions of the BZ was performed on the obtained self-consistent charge densities. The bulk moduli were evaluated by fitting the total energies at the different unit cell volumes on a Murnaghan equation of state.

The calculation of the electronic band structure, density of states (DOS) and dielectric function has been carried out by means of the self-consistent full potential linearized augmented plane wave method (FLAPW) in its scalar-relativistic version using the WIEN97 package.[19] The structural parameters of Ca$_2$Z in the orthorhombic and cubic phases fully optimized by USPP have been taken into consideration. We applied both LDA of Ceperly and Alder[17] and GGA of Perdew and Wang[18] similar to the case of USPP. Within the muffin-tin spheres, lattice harmonics with angular momentum l up to 10 are used to expand the charge density, potential and wave functions. The muffin-tin radii R_{mt} were set to 2.8, 2.2, 2.2, 2.5, and 2.5 a.u. for Ca, Si, Ge, Sn, and
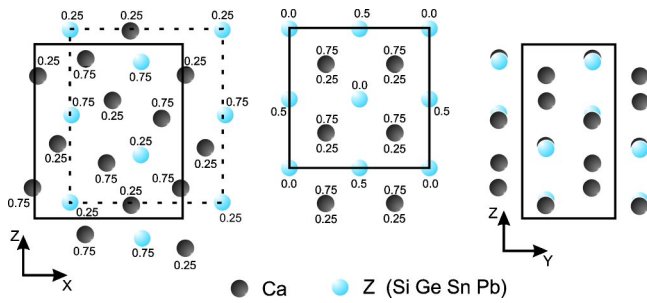
FIG. 1. (Color online) Projections of the orthorhombic structure on the (010) plane, of the cubic structure on the (001) plane, and of the orthorhombic structure on the (100) plane are in the left, middle, and right panels, respectively. The unit cell is marked by the solid line. The dashed line in left panel indicates a cell for better comparison with the cubic one. Fractional coordinates of atoms are also given in the left and middle panels. The calcium atoms are not separated into two chemically inequivalent sites for the orthorhombic structure.

Pb, respectively. We performed the self-consistent procedure with the energy cutoff constant $R_{mt}K_{max}=8$ and on meshes of 45 and 47 **k** points in the irreducible part of the BZ for the orthorhombic and cubic phases, respectively. Further increase in the cutoff value, basis set and **k**-point number did not lead to any noticeable changes in the eigenvalues. The integration on the BZ has been carried out by the tetrahedron method with Blöchl corrections. For a band structure representation we choose up to 40 **k** points for any high-symmetry direction. Dense meshes of 1200 **k** points (in the case of the orthorhombic structure) and 1059 **k** points (in the case of the cubic structure) were generated in the irreducible part of the BZ to compute total and projected DOS as well as dipole matrix elements. The random phase approximation was applied to calculate interband contribution to the imaginary part (ε_2) of the dielectric function and the Kramers-Kronig relation was employed to obtain the corresponding real part (ε_1).

III. RESULTS AND DISCUSSION

A. Structural properties

In Table I we summarize the lattice parameters, cohesion energies and bulk moduli of the Ca_2Z compounds both in the orthorhombic and cubic phases, as computed by USPP, in comparison with known experimental data. It is clearly seen that LDA sizably underestimates the lattice constants of the orthorhombic phase. Contrary to this, the results obtained by GGA, also underestimated, are very close to the experimental values. It is commonly believed that LDA overestimates the binding energy, so the underestimation of the lattice constants with respect to the experimental ones is likely to occur. On the other hand, GGA usually shows the opposite trends. However, in order to make a comparison between theoretically computed and experimentally measured lattice constants one should take into account the corresponding thermal expansion coefficient. Unfortunately the latter is unknown still assuming its positive value we find GGA to evaluate perfectly well the lattice parameters of orthorhom-
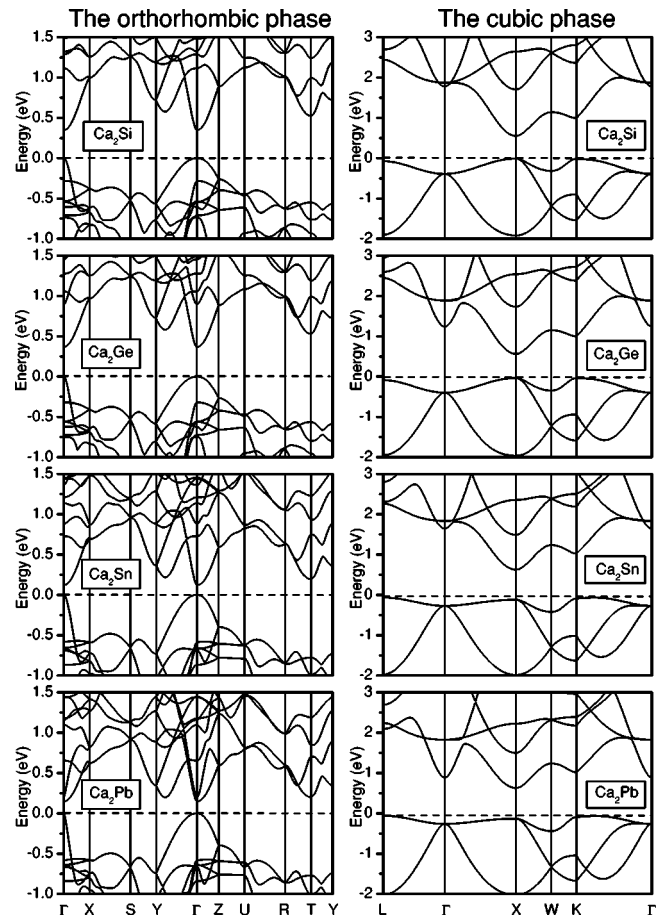
FIG. 2. The band structures of the orthorhombic and cubic phases of Ca_2Z calculated by FLAPW with GGA along some high-symmetry directions of the corresponding BZ at the energy region close to gap. Zero of the energy scale corresponds to the Fermi energy.

bic Ca_2Z. We also note that relaxed atomic positions are very close to the experimental ones[4,5] where the difference in the fractional coordinates is found to vary only in the third or fourth significant digit.

It is also evident that the cell equilibrium volumes of Ca_2Si and Ca_2Ge, Ca_2Sn, and Ca_2Pb both in orthorhombic and cubic phases are almost equal: the difference is less than 3% (Table I) as in the case of Mg_2Z.[2] However, the cell equilibrium volumes, for example, of Si and Ge are rather different (about 11%). This point can be understood by considering that Ca, having a bigger covalent radius with respect to Si, Ge, Sn, and Pb, defines unit cell dimentions of the Ca_2Z compounds. In fact, interatomic Ca-Ca distances in pure Ca (3.95 Å), in Ca_2Si, Ca_2Ge (3.55 Å) and in Ca_2Sn, Ca_2Pb (3.75 Å) are relatively close as if the Z atoms occupied emptiness in the Ca subcage. It should be noted here that the equilibrium volume of the cubic phase is predicted to be larger than the one of the orthorhombic phase.

Both LDA and GGA show the orthorhombic phase to be the stable phase for any Ca_2Z compound in agreement with experiment (Table I). The difference in the cohesion energy increases by moving from Ca_2Si to Ca_2Pb and it is comparable with values for some other pseudomorphic and metastable phases of transition metal silicides[20–22] and
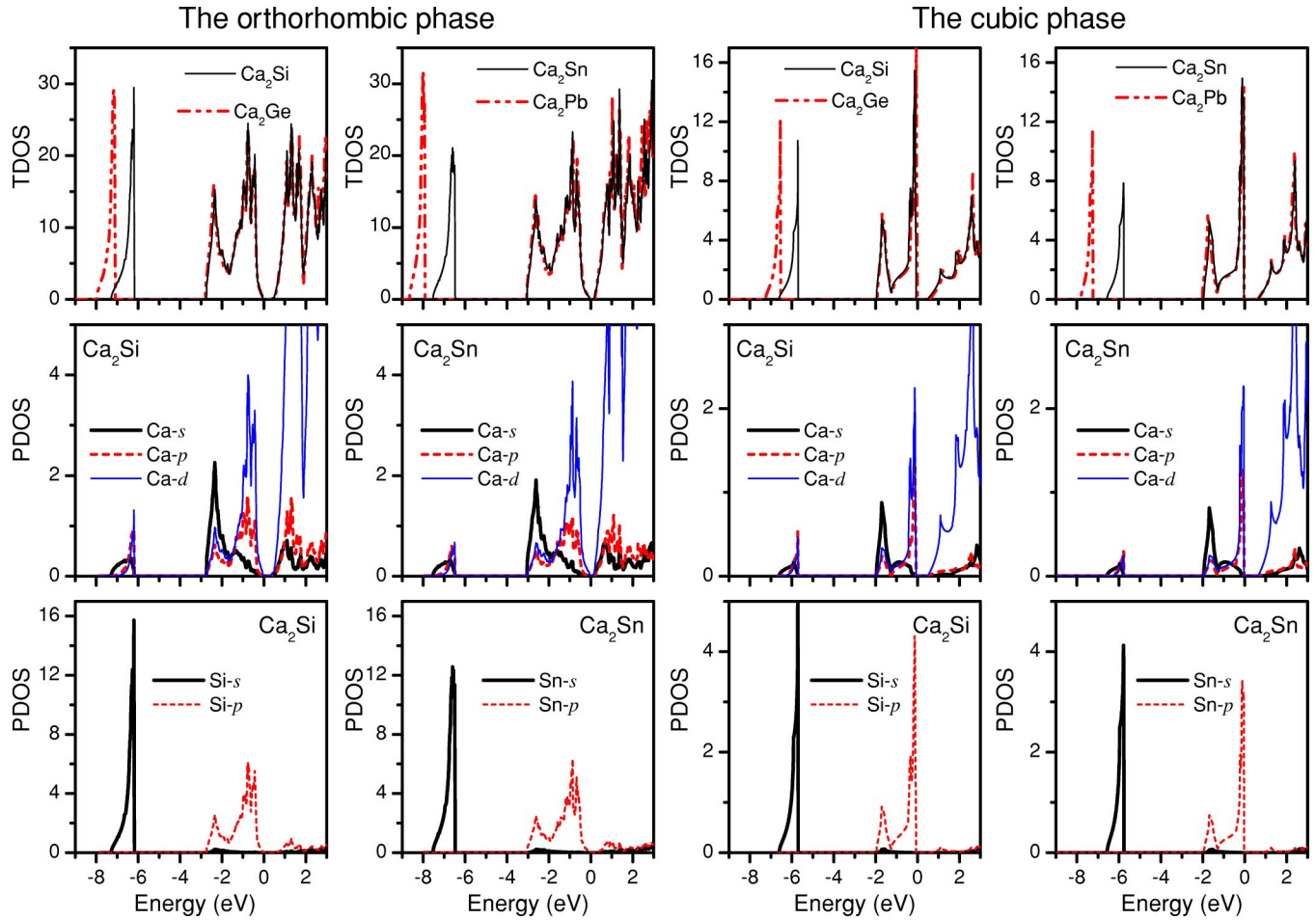
FIG. 3. (Color online) Total and projected density of states (TDOS and PDOS, respectively) in orthorhombic and cubic Ca_2Z computed by FLAPW with GGA. PDOSs are presented only for Ca_2Si and Ca_2Sn. In the case of orthorhombic phase the PDOS of the Ca atoms are summed over the two atomic types. TDOS and PDOS are in state/eV/cell. Zero of the energy scale corresponds to the Fermi energy.

germanides.[21] Dependence of the total energy with volume indicates the cubic phase to be lower in energy with respect to the orthorhombic one for all compounds only at volumes close to the corresponding equilibrium volume of the cubic phase, as has been reported in the case of Ca_2Si.[13] We also find that the bulk moduli of orthorhombic Ca_2Z are larger than the ones of the cubic phase (Table I). Their numerical estimates are comparable with that of Mg_2Si,[23] being several times smaller with respect to the values of some transition metal silicides[20,21] and germanides.[21]

B. Electronic structure

The band diagrams of Ca_2Z, computed by FLAPW with GGA, are presented in Fig. 2 demonstrating all compounds to be semiconductors. For the orthorhombic phase the energy gap, formed between the 16th and 17th bands, is characterized by a direct transition at the Γ point (Fig. 2, left panel). Its value is estimated to be 0.35, 0.37, 0.12, and 0.15 eV for Ca_2Si, Ca_2Ge, Ca_2Sn, and Ca_2Pb, respectively. These compounds have the same shape both of the top of the valence band with one pronounced maximum at the Γ point and of the bottom of the conduction band where minima at T and $0.2 \times Y$-Γ are some tens of meV higher in energy with re-

spect to the one in Γ. Just a different dispersion of the conduction 18th, 19th, and 20th bands at the Γ point can be observed with Z. The same band structures were obtained by USPP with GGA. Both methods using LDA agree in indicating that Ca_2Si displays the same topology of the bands close to the gap (0.12 eV) as in the case of GGA and no evidence of predicted semimetal properties[11] is found. Possible explanation of this fact can be the full structural optimization performed in our study and, moreover, our results with GGA are in perfect agreement with another psudopotential calculations for the silicide.[13]

In the case of the cubic phase only Ca_2Si and Ca_2Ge display a direct nature of the gap at the X point (0.56 and 0.60 eV, respectively) still the energy difference between the valence band maxima at X, K, and L is very small (Fig. 2, right panel). Ca_2Sn and Ca_2Pb show the conduction band minimum at the X point as in Ca_2Si and Ca_2Ge, whereas the valence band maximum is shifted to the L point being slightly higher in energy with respect to the ones at X and K (Fig. 2, right panel). The energy gaps of Ca_2Sn and Ca_2Pb are estimated to be 0.69 eV. We also note that cubic Ca_2Z and Mg_2Si, Mg_2Ge have almost the same shape of the bottom of the conduction band[24,25] while the sizeable rising of
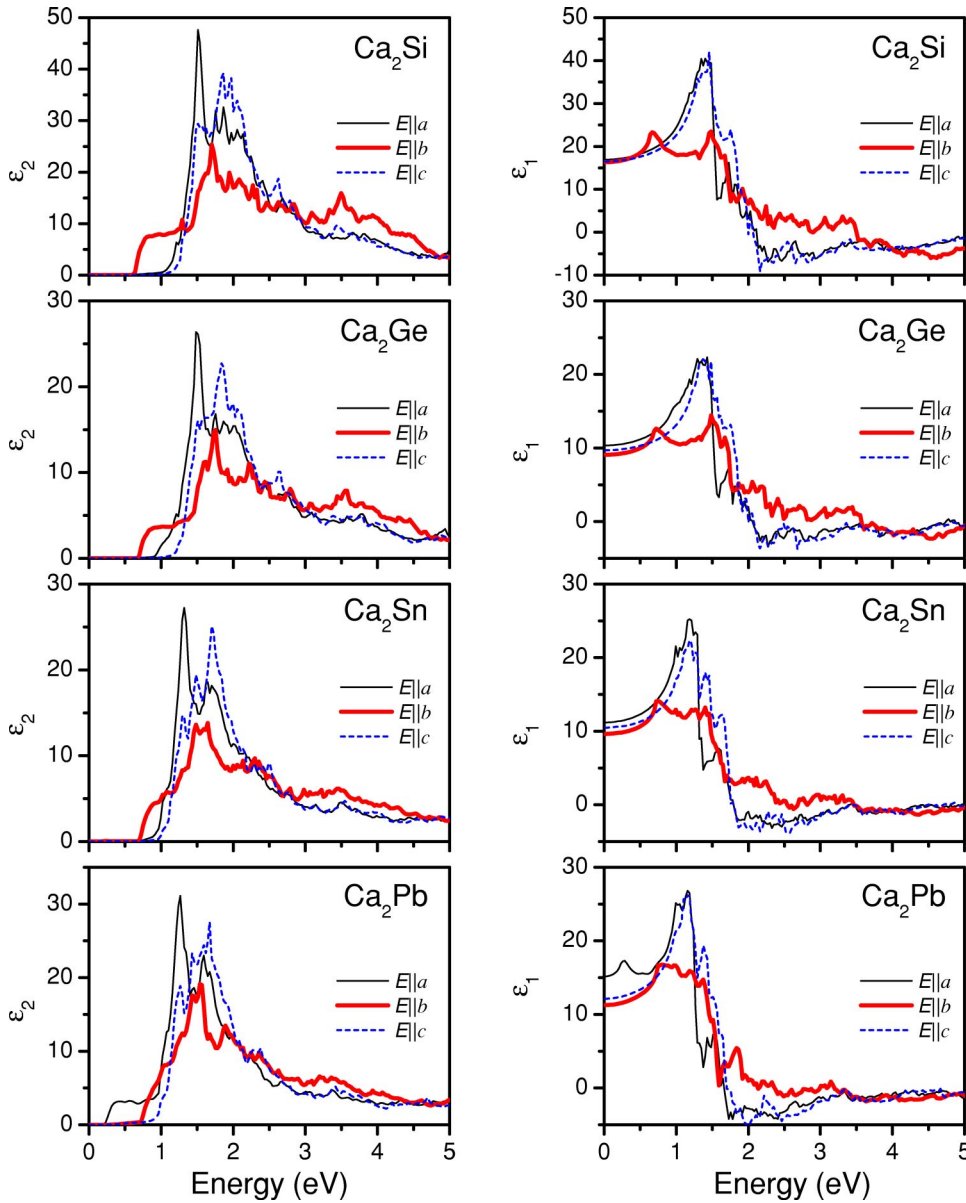
FIG. 4. (Color online) Imaginary (ε_2) and real (ε_1) parts of the dielectric function versus photon energy of orthorhombic Ca_2Z for the different light polarizations, as calculated by FLAPW with GGA.

the last valence band at L, X, and K is evident for the compounds of Ca.

It is clearly seen that Ca_2Si and Ca_2Ge, Ca_2Sn, and Ca_2Pb independently of the phase are characterized by almost the same value of the gap. Similar trend can also be traced in the case of Mg_2Z,[2] however, for Si, Ge, and Sn the gap shrinks quasilinearly. It seems to us that the gap value in Ca_2Z is strictly connected with the equilibrium volume which is almost equal for Ca_2Si and Ca_2Ge, Ca_2Sn, and Ca_2Pb as discussed in the previous section. The reason why the gap values of orthorhombic Ca_2Sn and Ca_2Pb are smaller with respect to the ones of orthorhombic Ca_2Si and Ca_2Ge, which is not the case for the cubic phase, will be given by considering the corresponding DOS.

The dependence of the total and projected DOS on energy of orthorhombic (cubic) Ca_2Z is presented in Fig. 3 displaying almost equal shape in the valence band with two well resolved parts. The first part is narrow, located around -7 eV (-6 eV) and composed mainly of the Z-s states. The gap of 3

eV (3.5 eV) separates it from the second part, a wider one, which extends from -3 eV (-2 eV) to the Fermi energy. Here bonding Z-p and Ca-spd sates play a dominant role. Nonbonding d-like states of the calcium atoms characterize the bottom of the conduction band. Our results in the case of orthorhombic Ca_2Si agree well with data obtained by *ab initio* calculations[11,13] and photoemission measurements.[11,12] Nevertheless, some differences in the DOS with respect to the phase and Z need more detail discussion. In fact, the narrow parts of Ca_2Si and Ca_2Ge, Ca_2Sn, and Ca_2Pb independently of the phase are shifted in energy while the broad ones and the bottom of the conduction bands almost coincide. This point can again be explained by the small difference in the equilibrium volumes, for instance, of Ca_2Si and Ca_2Ge with respect to the large one of Si and Ge. This, acting as a hydrostatical strain, is responsible for the displacement of the narrow band of the localized Z-s states which are not involved in the bond with Ca. Another feature in the DOS of the orthorhombic compounds is a parabolic

TABLE II. Orbital character and corresponding occupancy of the states of orthorhombic Ca$_2$Z at the Γ point. The occupancies (in %), and eigenvalues (eV) are given for Ca$_2$Si, Ca$_2$Ge, Ca$_2$Sn, and Ca$_2$Pb, respectively. Note that about 50 % of the charge are in the interstitial region.

		Valence band		Conduction band	
Band		15	16	17	18
Site/Energy		−0.28 −0.32 −0.58 −0.58	0.00 0.00 0.00 0.00	0.35 0.37 0.12 0.15	1.12 0.90 0.73 0.20
Ca1	s		(0.1 0.1 0.1 0.1)	(4.8 4.7 5.0 4.8)	(2.9 5.6 5.2 5.1)
	p	y(8.1 8.2 7.8 7.9)	x(0.3 0.3 0.4 0.2)	x(0.6 0.5 0.4 0.5)	x(0.1 0.2 0.1 0.1)
			z(0.1 0.1 0.2 0.1)	z(0.7 0.6 0.5 0.6)	z(4.2 0.1 3.5 0.1)
	d	xy(0.4 0.4 0.2 0.2)	$3z^2-r^2$(12.2 12.7 12.8 13.1)	$3z^2-r^2$(0.5 0.3 0.1 0.1)	$3z^2-r^2$(0.3 0.1 0.6 0.1)
		yz(2.4 2.1 1.7 1.6)	x^2-y^2(1.7 1.5 0.4 1.3)	x^2-y^2(10.4 10.7 10.8 9.8)	x^2-y^2(3.7 0.1 0.9 0.1)
			xz(1.4 1.2 1.7 2.0)	xz(0.6 0.6 0.6 0.1)	xz(0.3 0.3 0.1 0.3)
Ca2	s		(0.1 0.1 0.3 0.1)	(3.1 3.0 3.3 3.5)	(2.6 19.4 0.6 19.1)
	p	y(8.2 8.4 8.3 8.3)	x(1.9 1.9 1.3 1.2)	x(0.6 0.6 0.7 0.4)	x(2.3 0.1 4.0 0.1)
			z(0.1 0.1 0.3 0.3)	z(0.3 0.3 0.1 0.3)	z(1.2 1.1 1.0 0.5)
	d	xy(0.4 0.4 0.4 0.3)	$3z^2-r^2$(3.8 3.8 4.0 4.8)	$3z^2-r^2$(0.3 0.3 0.9 0.3)	$3z^2-r^2$(9.7 0.7 9.8 0.6)
		yz(0.3 0.3 0.1 0.1)	x^2-y^2(1.4 1.8 3.3 1.4)	x^2-y^2(20.8 20.8 16.2 18.1)	x^2-y^2(1.6 1.2 5.5 0.6)
			xz(1.1 0.9 0.3 0.6)	xz(4.1 4.4 4.2 4.0)	xz(15.8 0.1 9.9 0.2)
Z	s		(0.1 0.1 0.1 0.1)	(0.1 0.1 0.1 0.1)	(1.4 25.2 2.2 22.3)
	p	y(31.2 35.7 32.1 29.1)	x(30.3 34.9 30.5 28.2)	x(0.1 0.1 0.8 0.1)	x(0.5 0.3 0.1 0.3)
			z(0.1 0.1 0.1 0.1)	z(0.6 0.7 0.7 0.7)	z(3.7 0.5 3.6 0.6)
	d	xy(0.1 0.1 0.1 0.1)	$3z^2-r^2$(0.2 0.2 0.2 0.2)	$3z^2-r^2$(0.1 0.1 0.1 0.1)	$3z^2-r^2$(0.6 0.1 1.4 0.1)
		yz(0.2 0.2 0.1 0.1)	x^2-y^2(0.1 0.1 0.1 0.1)	x^2-y^2(2.3 2.2 2.6 2.4)	x^2-y^2(0.1 0.1 0.1 0.1)
			xz(0.1 0.1 0.1 0.1)	xz(0.2 0.1 0.1 0.1)	xz(0.9 0.1 0.2 0.1)

reduction of the top of the valence band indicating a Z-Ca p-d hybridization as in the case of Ru$_2$Si$_3$.[26] This is more pronounced for Ca$_2$Sn and Ca$_2$Pb because of the larger extent of the Sn 5p and Pb 6p orbitals, to be compared to the Si 3p and Ge 4p ones, and their overlap with Ca-d states, resulting in a gap reduction. On the contrary, linear, almost perpendicular shape, which can be attributed to the antibonding states, is evident for the cubic phase and here the gap values are relatively close.

C. Optical properties

The ε_2 and ε_1 dependencies on the photon energy, shown in the Fig. 4, demonstrate a sizable anisotropy of the optical properties of the Ca$_2$Z compounds in the orthorhombic structure. It is clearly seen that the $E\|a$ and $E\|c$ spectra are very similar on the contrary to the $E\|b$ ones. Moreover, the former curves in the case of ε_2 are very close in shape to those of cubic Mg$_2$Si and Mg$_2$Ge.[25] The big similarity in the optical functions in the case of the a and c light polarizations can be understood by taking into account that the projection on the (010) plane in the orthorhombic structure (the case of $E\perp b$) corresponds to the one of the (001) plane in the cubic structure (see discussion to Fig. 1).

Some low energy features in the presented optical spectra of orthorhombic Ca$_2$Z (Fig. 4) such as an abrupt threshold in the ε_2 curves at about 0.7 eV in the case of the b light polarization and a strong ε_2 increase at 0.20 eV for $E\|a$ only in the case of Ca$_2$Pb require more detail investigation. In order to identify them with the interband transitions we have examined the dipole matrix elements of the various pairs of

bands and corresponding orbital characters of the states. The valence band maximum for all Ca$_2$Z is almost characterized by the Ca-d and Z-p states, whereas the d-states of the calcium atoms dominate in the conduction band minimum (see Table II). The 16→17 transition at the Γ point has main contributions from the following matrix elements: $\langle 3z^2-r^2|z|z\rangle$, $\langle xz|x|z\rangle$ on the Ca1 site, $\langle x|x|x^2-y^2\rangle$, $\langle x|z|xz\rangle$ on the Ca2 site, and $\langle y|y|x^2-y^2\rangle$ on the Z site. Still their numerical estimates resulted in small values. On the contrary, the contributions $\langle y|y|x^2-y^2\rangle$ from the Ca1 and Ca2 sites to the 15→17 transition at Γ are found to be large, and this, in turn, gives rise to the strong absorption at about 0.7 eV for
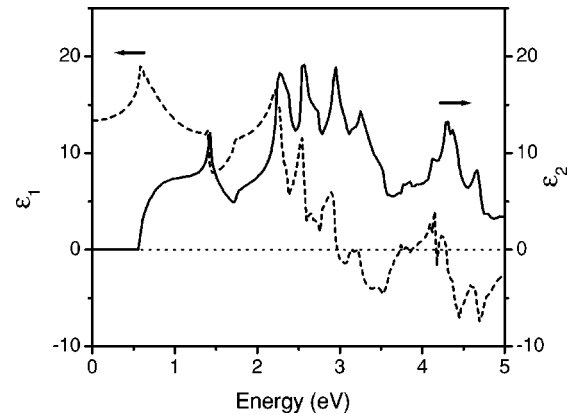
FIG. 5. Imaginary (ε_2) and real (ε_1) parts of the dielectric function (marked by the solid and dashed lines, respectively) versus photon energy, as calculated by FLAPW with GGA, in the case of cubic Ca$_2$Si.

$E\|b$ (see Fig. 4). This big difference in intensity of the 16 $\rightarrow$17 and 15$\rightarrow$17 transitions stems from the small admixture of the Ca-p states in the 16th band with respect the one in the 15th band (Table II). The feature at 0.20 eV for Ca$_2$Pb can be ascribed to the 16$\rightarrow$18 transition at Γ due to the sizable contribution $\langle x|x|s\rangle$ from the Pb site.

The most striking peculiarity in optical spectra of cubic Ca$_2$Si is a rapid start of ε_2 at 0.56 eV (see Fig. 5) manifesting the high value of the oscillator strength of the first direct transition at the X point. The analysis of the states indicates that the valence band maximum and conduction band minimum at this point are mainly composed of Ca-p, Si-p and Ca-d, Si-d, respectively. Similar results were also obtained in the case of Ca$_2$Ge, Ca$_2$Sn, and Ca$_2$Pb in the cubic structure.

IV. CONCLUSIONS

The performed investigation points out the orthorhombic phase to be the stable phase being lower in total energy with respect to the cubic one for all Ca$_2$Z compounds. The direct nature of the gap is predicted in the case of orthorhombic Ca$_2$Z still the first direct transition displays the low value of oscillator strength. In the case of Ca$_2$Z in the cubic structure the last valence band shows a small dispersion with several maxima close in energy and this, in turn, gives rise to quasidirect or competitive direct-indirect character of the gap. Actually we do not want to speculate about the gap value of these Ca$_2$Z compounds. It is well known that density functional methods within LDA or GGA usually underestimate the value of the band gap and *ab initio* quasiparticial calculations are desirable. Still all-electron full-potential projector augmented wave method within the GW approximation predicts a smaller energy gap for cubic Mg$_2$Si and Mg$_2$Ge with respect to the experiment.[24,25] On the other hand, one has to be careful with the gap estimates in Ca$_2$Si (1.90 eV), Ca$_2$Sn (0.90 eV), and Ca$_2$Pb (0.46 eV) by resistivity measurements in Ref. 10 because of the problems in the crystal structure determination. Optical measurements on high quality samples are necessary in order to provide information about their band gap values. Nevertheless, in the case of orthorhombic Ca$_2$Z the revealed sizable anisotropy in optical functions ($E\|b$ and $E\perp b$) and the low value of oscillator strength of the first direct transition will be useful in interpretation of experimental optical spectra. Finally, we suggest that Ca$_2$Si and Ca$_2$Ge in the cubic structure having attractive optical properties can be grown on a suitable cubic substrate, such as a diamond because of the relatively small lattice mismatch (less than -1% with respect to the doubled lattice constant of diamond).

*Electronic address: migas@mater.unimib.it

[1] *Semiconducting Silicides*, edited by V. E. Borisenko (Springer, Berlin, 2000).

[2] *Silicides:Fundamentals and Applications*, edited by L. Miglio and F. d'Heurle (World Scientific, Singapore, 2000).

[3] A. K. Ganguli, A. M. Guloy, and J. D. Corbett, J. Solid State Chem. **152**, 474 (2000).

[4] P. Eckerlin and E. Wölfel, Z. Anorg. Chem. **280**, 321 (1955).

[5] P. Eckerlin, E. Leicht, and E. Wölfel, Z. Anorg. Allg. Chem. **307**, 145 (1961).

[6] P. Manfrinetti, M. L. Fornasini, and A. Palenzona, Intermetallics **8**, 223 (2000).

[7] A. Palenzona, P. Manfrinetti, and M. L. Fornasini, J. Alloys Compd. **312**, 165 (2000).

[8] G. Buzzone and F. Merlo, J. Less-Common Met. **48**, 103 (1976).

[9] A. Palenzona, P. Manfrinetti, and M. L. Fornasini, J. Alloys Compd. **345**, 144 (2002).

[10] G. Busch, P. Junod, U. Katz, and U. Winkler, Helv. Phys. Acta **27**, 193 (1954).

[11] O. Bisi, L. Braicovich, C. Carbone, I. Lindau, A. Iandelli, G. L. Olcese, and A. Palenzona, Phys. Rev. B **40**, 10 194 (1989).

[12] C. Chemelli, M. Sancrotti, L. Braicovich, F. Ciccacci, O. Bisi, A. Iandelli, G. L. Olcese, and A. Palenzona, Phys. Rev. B **40**, 10 210 (1989).

[13] Y. Imai and A. Watanabe, Intermetallics **10**, 333 (2002).

[14] G. Kresse and J. Hafner, Phys. Rev. B **49**, 14 251 (1994).

[15] G. Kresse and J. Futhmüller, Comput. Mater. Sci. **6**, 15 (1996).

[16] G. Kresse and J. Futhmüller, Phys. Rev. B **54**, 11 169 (1996).

[17] J. Perdew and A. Zunger, Phys. Rev. B **23**, 5048 (1981).

[18] Y. Wang and J. P. Perdew, Phys. Rev. B **44**, 13 298 (1991).

[19] P. Blaha, K. Schwarz, and J. Luitz, WIEN97, Vienna University of Technology 1997 [improved and updated Unix version of the original copyrighted WIEN code, which was published by P. Blaha, K. Schwarz, P. Sorantin, and S.B. Trickey, Comput. Phys. Commun. **59**, 399 (1990)].

[20] E. G. Moroni, W. Wolf, J. Hafner, and R. Podloucky, Phys. Rev. B **59**, 12 860 (1999).

[21] D. B. Migas, L. Miglio, V. L. Shaposhnikov, and V. E. Borisenko, Phys. Status Solidi B **231**, 171 (2002).

[22] D. B. Migas and L. Miglio, Appl. Phys. Lett. **79**, 2175 (2001).

[23] J. L. Corkill and M. L. Cohen, Phys. Rev. B **48**, 17 138 (1993).

[24] B. Arnaud and M. Alouani, Phys. Rev. B **62**, 4464 (2000).

[25] B. Arnaud and M. Alouani, Phys. Rev. B **64**, 033202 (2001).

[26] W. Wolf, G. Bihlmayer, and S. Blügel, Phys. Rev. B **55**, 6918 (1997).